

Control of progenitor cell number by mitogen supply and demand

Paul van Heyningen, Andrew R. Calver* and William D. Richardson

Background: Much is known about how cell proliferation is controlled at the single cell level, but much less about the control of cell numbers in developing populations. Cell number might be determined by an intracellular division limiter or, alternatively, by the availability of mitogens or other factors outside the cell. We investigated the relative importance of intracellular and extracellular controls for one well-defined population of neural precursor cells, namely the glial progenitors that give rise to oligodendrocytes in the mouse spinal cord.

Results: We found by cumulative BrdU labeling *in vivo* that the progenitor cell division cycle slows down markedly as their numbers increase during embryogenesis. When cultured in saturating PDGF, the main mitogen for these cells, their cell cycle accelerated and was independent of their prior rate of division *in vivo*. This shows that mitogens are limiting *in vivo*, and suggests that division normally slows down because the PDGF concentration declines. In PDGF-transgenic mice, cell number was proportional to the PDGF supply and apparently unsaturable; at ten times the normal rate of supply, cell number was still increasing but the animals were no longer viable.

Conclusions: Progenitor cell proliferation in the embryo is limited by environmental factors, not a cell-intrinsic mechanism. The linear relationship between PDGF supply and final cell number strongly suggests that cells deplete the mitogenic activity in their environment at a rate proportional to the total number of cells. The cells might simply consume the available PDGF or they might secrete autocrine inhibitors, or both.

Background

The ultimate size of an organism is determined by the number of cells that develop in its various tissues and organs. Cell numbers are determined by the combined effects of cell proliferation, differentiation, and long-term survival, each of which is regulated by interactions between cells and their local environment. We do not have a clear idea of how these controls, which operate on individual cells, are integrated at a population level to deliver the appropriate final number and density of cells. It is possible that each cell has an inbuilt limit on the number of replicative cycles it can undergo or the length of time it can remain in cycle, and cells automatically stop dividing and differentiate when they reach this limit. Alternatively, the limit could be set by the amounts of mitogenic or antiproliferative factors in the local environment [1, 2].

We are trying to understand how cell numbers are controlled by studying a population of neural progenitor cells that gives rise to oligodendrocytes, the myelin-forming cells of the central nervous system (CNS). Oligodendrocyte progenitors are amenable to studies of proliferation control, first because there are lineage markers that allow them to be visualized and counted *in situ*, second because they can be grown, labeled, and counted readily *in vitro*,

Address: Wolfson Institute for Biomedical Research and Department of Biology, University College London, Gower Street, London WC1E 6AE, UK.

Present address: *Department of Neuropharmacology, GlaxoSmithKline, New Frontiers Science Park North, Third Avenue, Harlow, Essex CM19 5AW, UK.

Correspondence: Bill Richardson
E-mail: w.richardson@ucl.ac.uk

Received: 16 November 2000

Revised: 15 December 2000

Accepted: 11 January 2001

Published: 20 February 2001

Current Biology 2001, 11:232–241

0960-9822/01/\$ – see front matter

© 2001 Elsevier Science Ltd. All rights reserved.

and third as it is known that the major mitogen for these cells *in vivo* is platelet-derived growth factor (PDGF), the biochemistry of which is relatively well understood.

We previously reported that the oligodendrocyte progenitor cell cycle slows down markedly as their numbers increase in the embryonic spinal cord [3]. This behavior is common to other types of embryonic precursors. For example, the division cycle of pluripotent precursors in the embryonic rat cerebral cortex slows from ~ 8 to ~ 24 hr during cortical neurogenesis [4]. Determining the cause of this dynamic cell cycle behavior will be crucial for understanding how final cell number is controlled during development.

We show here that if spinal cord cells are dissociated and cultured in the presence of saturating concentrations of PDGF, the oligodendrocyte progenitor cells cycle rapidly irrespective of how slowly they were cycling *in vivo* prior to dissociation. Therefore, the mechanism that causes the progenitor cell cycle to slow down *in vivo* is not cell intrinsic, but rather involves a change in the extracellular environment of the developing CNS. By manipulating PDGF expression in the spinal cords of transgenic mice, we show that the upper limit on progenitor cell number

is set in direct proportion to the level of *PDGF* transcripts (rate of production of PDGF). The linear range extends from practically no PDGF expression (in *PDGF-A* null mice) to many times normal (in transgenic *PDGF-A* over-expressers) with no sign of impending saturation. The simplest explanation is that no matter what the rate of PDGF production, cells proliferate until the PDGF supply becomes limiting. When the rate at which cells consume PDGF approaches the rate of supply, competition for PDGF intensifies and its extracellular concentration drops, causing the cell division cycle to slow down and preventing a further increase in cell number.

Results

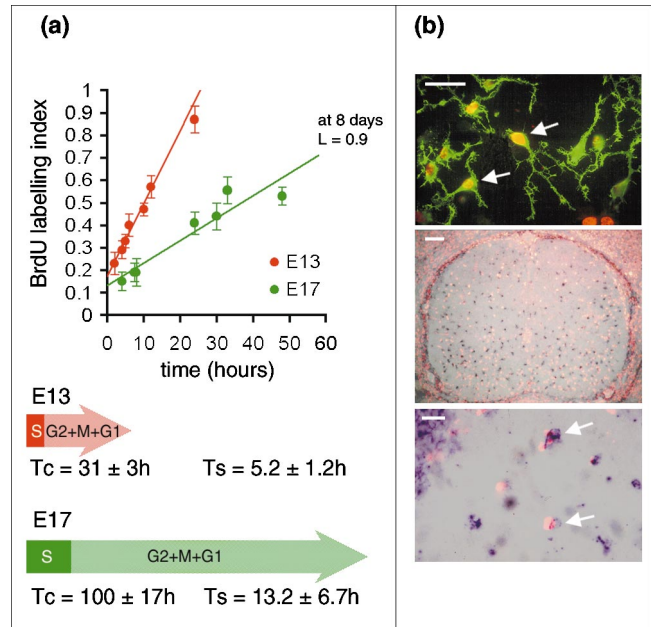
The oligodendrocyte progenitor cell cycle slows down markedly before birth

In the rodent spinal cord, oligodendrocyte progenitors can be visualized by immunohistochemistry and/or in situ hybridization for PDGF α receptors (*PDGFR α*) and the proteoglycan NG2 [5–7]. *PDGFR α* -positive progenitors first appear in the ventral neuroepithelium near the floor plate on embryonic day 12.5 (E12.5) in the mouse [3]. Subsequently, they proliferate and migrate throughout the cross section of the cord before differentiating into oligodendrocytes. We previously conducted a cumulative BrdU-labeling study in vivo and concluded that the cell division rate of oligodendrocyte progenitors slows down dramatically (from ~ 8 to ~ 24 hr) between E13 and birth [3]. We have now repeated that study and confirm the general conclusion that cell division slows down. We found, however, that our previous cell cycle times were seriously underestimated. We found instead that the progenitor cell cycle slows from ~ 30 to ~ 100 hr within the same period (Figure 1; see Materials and methods for details). There are methodological differences between this and our earlier study, notably the use of osmotic minipumps rather than sequential injections for BrdU delivery. In trial experiments, however, we found that both methods yielded comparable results. We also compared the following two methods of scoring BrdU-labeled progenitors: combined BrdU immunodetection and *PDGFR α* in situ hybridization on tissue sections, and double immunolabeling for BrdU and NG2 in dissociated cell cultures (Figure 1). Again, both methods gave comparable data. Therefore, while we do not fully understand the reasons for our earlier error, we are confident that our revised (longer) cell cycle estimates are reliable, and should supersede those of Calver *et al.* (see Discussion) [3].

Slowing of the cell cycle reflects a changing mitogenic environment in vivo

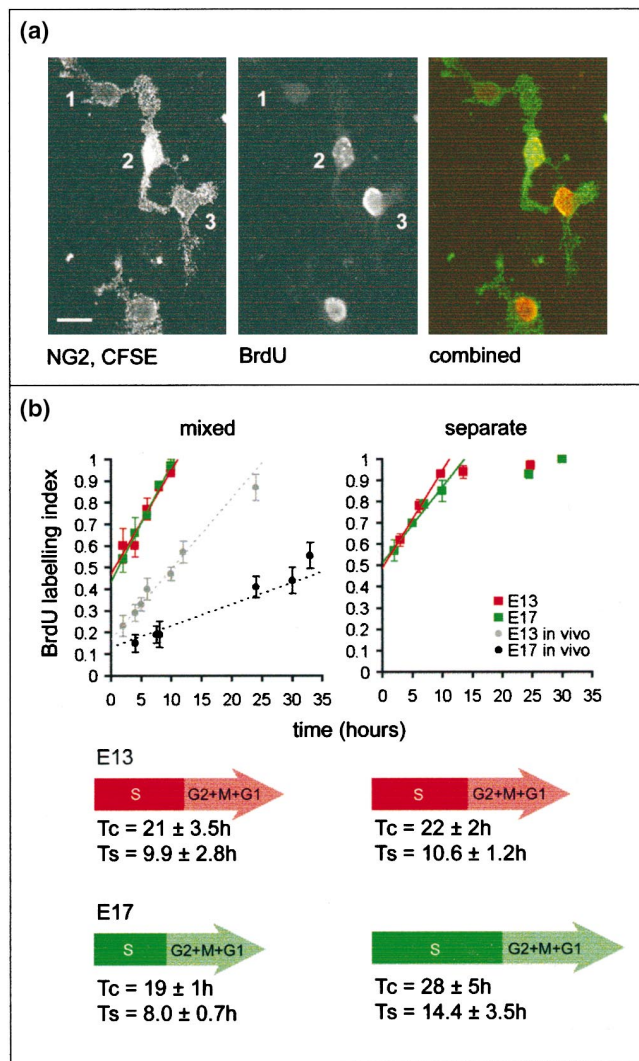
We asked whether the slowdown in the cell cycle noted above resulted from an intrinsic change in the mitogenic responsiveness of progenitor cells or, alternatively, a change in their extracellular environment. We dissociated spinal cord cells from E13 and E17 mice and placed them in culture, either separately or mixed, in a medium con-

Figure 1

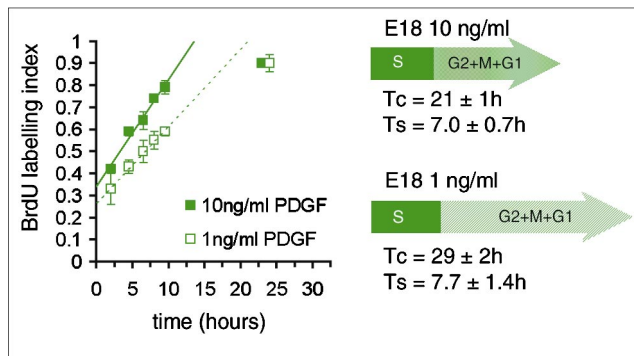


Cumulative BrdU labeling of embryonic oligodendrocyte progenitors in vivo. **(a)** E13 and E17 mouse embryos were BrdU labeled by implanting an osmotic minipump in the mother. After the desired time, embryonic spinal cord cells were dissociated, cultured overnight, and immunolabeled for NG2 proteoglycan and BrdU. The BrdU labeling index was plotted against time. Total cell cycle time (T_c) and S phase time (T_s) were calculated from the line of best fit and are depicted graphically. In this and subsequent figures, the total length of the arrow represents T_c and the block of solid color represents T_s . The cells cycle more than three times slower at E17 than at E13. **(b)** Comparison of methods for calculating the oligodendrocyte progenitor labeling index after BrdU labeling in vivo. Top panel: dissociated spinal cord cells were cultured overnight and immunolabeled with anti-NG2 and anti-BrdU. Arrows show two ($NG2^+$, $BrdU^+$) progenitors. Middle and bottom panels: a transverse section of an embryonic spinal cord was subjected to in situ hybridization with a probe against *PDGFR α* followed by immunodetection of BrdU. Immunofluorescence micrographs are superimposed on the corresponding in situ hybridization images. Arrows in the bottom panel show two (*PDGFR α* $^+$, $BrdU^+$) progenitors. The cell culture method and the in situ method gave similar BrdU labeling indices, so the simpler culture method was used for all experiments reported in this paper. The scale bars represent 10 μm (top and bottom) and 100 μm (middle).

taining BrdU (10 μM) and a saturating amount of recombinant PDGF-AA (10 ng/ml). After various times in vitro, we fixed the cells and immunolabeled them with antibodies against BrdU and NG2 to visualize progenitors that had undergone DNA synthesis in culture. We could distinguish E13 and E17 cells in the mixed cultures because we prelabeled one of the populations with a fluorescent membrane-permeable dye (CFSE, Molecular Probes) before plating (Figure 2). These cumulative BrdU-labeling experiments showed that there is no intrinsic difference between E13 and E17 cells in their mitogenic response to saturating PDGF in vitro and that both populations of progenitors cycled much faster in vitro, in saturating

Figure 2

Cumulative BrdU labeling of oligodendrocyte progenitors in vitro. **(a)** Dissociated E13 spinal cord cells were prelabeled with the fluorescent dye CFSE (see Materials and methods) before they were mixed with unlabeled E17 cells and cultured overnight. BrdU was then added for various times before fixing and immunolabeling with anti-NG2 and anti-BrdU. The CFSE and fluorescein signals are both green, but can be distinguished because CFSE is in the cytoplasm whereas NG2 is on the cell surface. Numbered cells: (1) an (NG2⁺, BrdU⁻, CFSE⁻) E17 progenitor, (2) an (NG2⁺, BrdU⁺, CFSE⁺) E13 progenitor, and (3) an (NG2⁺, BrdU⁺, CFSE⁻) E17 progenitor. The scale bar represents 10 μ m. **(b)** The BrdU labeling index was plotted against time for E13 and E17 cells (see key) in mixed-age cultures (left graph) and separate cultures (right graph). Tc and Ts were calculated from the lines of best fit and are shown graphically. The in vivo labeling data from Figure 1 are also shown for comparison. Points that appear to be on the plateau were not included when calculating the line of best fit. There is no significant difference between the cell cycles of E13 and E17 cells, unlike the situation in vivo. Note also that the division rate is speeded up in vitro compared to in vivo for both E13 and E17 cells.

Figure 3

PDGF concentration controls progenitor cell cycle time in vitro. Spinal cords from E18 embryos were dissected and cultured overnight in 10 ng/ml or 1 ng/ml PDGF-AA. BrdU was added and the cumulative labeling index was determined. The oligodendrocyte progenitor cell cycle was significantly longer at 1 ng/ml than at 10 ng/ml PDGF. Variation was largely in the G2-M-G1 phases of the cycle.

PDGF, than they did in vivo prior to dissociation (Figure 2). We conclude from the latter observation that PDGF is limiting for cell division in vivo at both E13 and E17. There might also be an inhibitory activity in vivo that is lost when the cells are placed in culture. The reason the cell cycle slows down in vivo between E13 and E17 is not because the cells' inherent ability to respond to mitogens decreases, but because there is less mitogenic activity in the extracellular environment. That is, the PDGF concentration falls and/or a putative inhibitory activity rises.

Progenitor cell cycle time depends on PDGF concentration

To test the principle that a falling PDGF concentration might slow the progenitor cell cycle in vivo, we measured the cell cycle time of E18 progenitor cells cultured in either 10 ng/ml or 1 ng/ml PDGF. In both saturating and subsaturating PDGF concentrations, the progenitors behaved as uniform populations of cycling cells; the proportion of BrdU-labeled cells increased linearly with time until almost all of the cells were labeled (Figure 3). The cell division rate depended on PDGF concentration, however. In 10 ng/ml PDGF, the cell cycle time was 21 ± 1 hr, whereas in 1 ng/ml PDGF it was 29 ± 2 hr (Figure 3). Even the latter time is much shorter than is observed in vivo at E17 (100 ± 17 hr), suggesting that the effective PDGF concentration might fall significantly below 1 ng/ml in vivo. In any case, this experiment demonstrates that the falling cell division rate in vivo could potentially be caused by a dwindling PDGF concentration. Note that the length of S phase was not affected by the PDGF concentration in vitro, consistent with previous studies on cultured fibroblasts. A similar dependence of cell cycle time on PDGF concentration was also observed for E14 progenitors (data not shown).

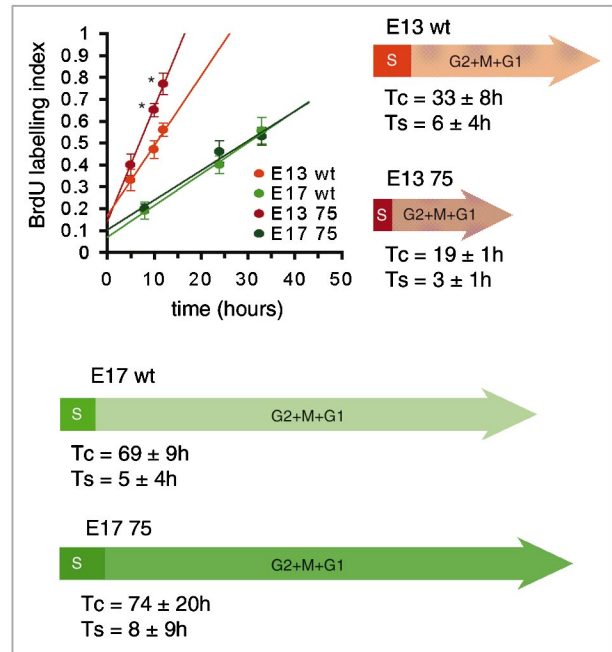
Cell number is controlled by the PDGF supply in a linear, unsaturable fashion

Cell-intrinsic mechanisms do not appear to be responsible for limiting progenitor cell number during normal embryonic development (see previous two paragraphs). It might be expected that there would be some inbuilt limit on proliferation as a fail-safe device, however, in case mitogenic activity in the environment were deregulated somehow during development or neoplasia. We imagined that a cell-intrinsic mechanism would kick in to halt cell division if we were to induce extreme hyperproliferation of progenitor cells by elevating PDGF expression beyond some critical point *in vivo*. We tested this idea by overexpressing PDGF in transgenic mice.

We previously described a line of transgenic mice that expresses human PDGF-A in the CNS under the control of the neuron-specific enolase promoter (*NSE-PDGF-A* mice) [8]. This line (#75) developed greater than normal numbers of oligodendrocyte progenitors in the spinal cord, approximately three times more in hemizygotes and seven times more in homozygotes [3]. The cell cycle slowed down and the cell number reached a stable upper limit (steady state) just as in wild-type mice, except that the final cell number and density were higher in the transgenics. Cell division was faster in the transgenics at early times (E13), accounting for the greater number of cells at steady state (Figure 4) [3]. At later times (E17) however, cell division in the transgenics slowed to the same rate as the wild type (Figure 4) [3]. This suggests that the extracellular PDGF concentration at steady state is the same in the transgenics as in the wild type. This might seem counterintuitive, but it must be borne in mind that the transgenics express not only more PDGF, but also more PDGF receptors (because they have more progenitor cells), introducing the idea that progenitor cell proliferation might always be limited by the relative rates of PDGF supply and demand (see Discussion).

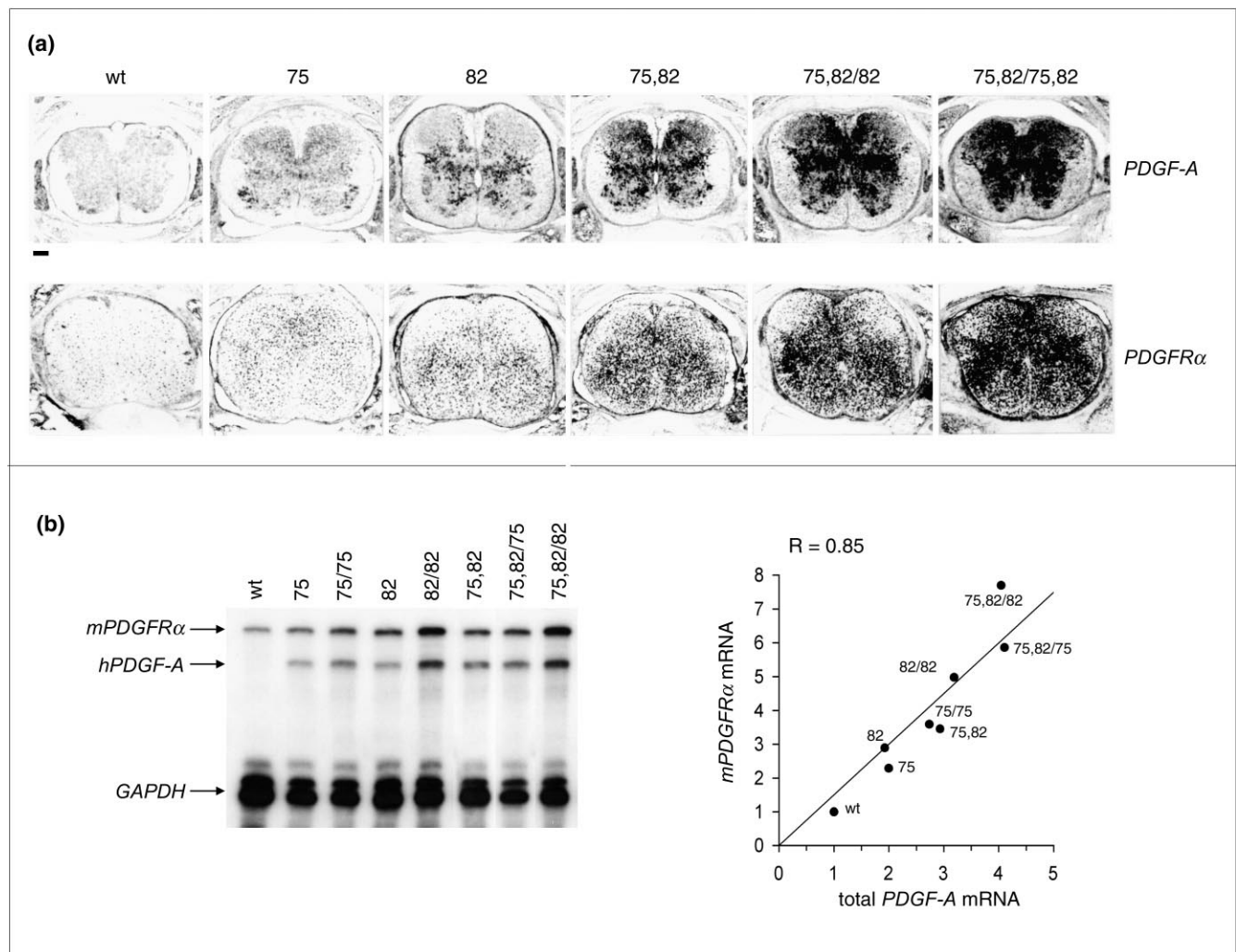
We increased PDGF expression still further by interbreeding line #75 with another line of *NSE-PDGF-A* mice (#82) to generate offspring with up to four *PDGF-A* transgene loci in addition to their two endogenous genes. Our breeding regimen could possibly have generated nine different genotypes of which we found eight (Figure 5). We visualized *PDGF-A* expression by *in situ* hybridization with a human cDNA probe that binds both endogenous (mouse) and transgenic (human) *PDGF-A* transcripts. In parallel, we visualized oligodendrocyte progenitor cells with a probe against mouse *PDGFR α* . By eye, there appeared to be a close correlation between the abundance of PDGF ligand and receptor transcripts at E15, even at the highest levels of *PDGF-A* expression (Figure 5a). We quantified mRNA abundance in newborn mice by RNase protection (see Materials and methods) and confirmed this visual impression; there was an approximately linear

Figure 4



PDGF overexpression in transgenic mice delays slowing of the progenitor cell cycle *in vivo*. E13 and E17 embryos from wild-type (wt) female mice mated with hemizygous *NSE-PDGF-A* transgenic (line #75) males were BrdU labeled *in vivo*. Spinal cord cells from each embryo were dissociated and cultured individually on coverslips. The embryos were genotyped retrospectively. Each data point represents the mean \pm SD for at least three and up to six embryos. Asterisks (*) mark data points for which the difference between wild type and #75 is statistically significant (Student's *t* test; $p < 10^{-6}$). The data show that transgenic progenitors cycle faster than wild-type progenitors at E13. By E17, the division cycle slows down to approximately the same rate (~ 70 hour cycle) in both wild-type and transgenic mice, however. Tc and Ts, estimated from lines of best fit, are illustrated graphically.

relationship between *PDGF-A* and *PDGFR α* transcript levels (Figure 5b). Because we showed that *PDGFR α* transcript levels accurately reflect the number of *PDGFR α* -expressing cells (see Figure 7 and Materials and methods), we conclude that cell number is directly proportional to *PDGF-A* expression over the full range of genotypes examined. This unexpected result is explicable only if *PDGF-A* mRNA abundance directly determines the rate of synthesis and secretion of the PDGF-A protein, which in turn determines the number of progenitor cells at steady state. It is striking that there is no obvious sign of the PDGF dose–response plot approaching saturation *in vivo* (Figure 5b). Therefore, there appears not to be any cell-intrinsic limit on proliferation even when the cell number is amplified more than 10-fold (Figure 5a). At this extreme, the mice displayed spinal curvature and vertebral deformities, and did not survive the first postnatal week [9].

Figure 5

Progenitor cell number in newborn mice is proportional to the PDGF supply. **(a)** Spinal cord sections of E15 wild-type and transgenic *NSE-PDGF-A* mouse embryos with the genotypes shown were subjected to in situ hybridization with probes against *PDGFRα* and *PDGF-A*. To allow a fair comparison of the sections, in situ hybridization reactions were carried out at the same time and photographed under identical conditions. The numbers of *PDGFRα*⁺ progenitor cells rise in parallel with *PDGF-A* expression, even at the highest levels of expression. The scale bar represents 150 μm. **(b)** mRNAs encoding mouse *PDGFRα* and transgene-derived human *PDGF-A* (*hPDGF-A*) were

quantified in newborn mice by RNase protection. *PDGFRα* transcript levels provide an accurate reflection of the number of *PDGFRα*-positive cells (see Figure 7). The relative amount of endogenous *PDGF-A* was estimated in a separate experiment (data not shown) to be equivalent to the contribution from one transgenic allele (#75). This was added to each transgenic contribution before plotting total *PDGF-A* versus *PDGFRα* (normalized to wt = 1). The dose response is approximately linear (correlation coefficient R = 0.85). Thus, progenitor cell number is directly proportional to the rate of PDGF supply, even at very high levels of PDGF overexpression.

We also examined the effect of reducing mitogen expression in *PDGF-A* knockout mice [10]. As reported before [3, 11], homozygous knockouts had very few *PDGFRα*-expressing progenitor cells in their spinal cords (<10% normal). Heterozygous *PDGFRα* knockouts had close to half the normal number (Figure 6). Therefore, the linear relationship between *PDGF-A* expression and the final cell number holds for reduced as well as for elevated levels of *PDGF* expression (Figure 6). Note that progenitor cell densities were sufficiently low in the sections of Figure 6 that they could be counted directly from the in situ

hybridization images rather than indirectly by *PDGFRα* mRNA abundance as in Figure 5. This confirms and reinforces the conclusion that cell number and PDGF supply are directly proportional.

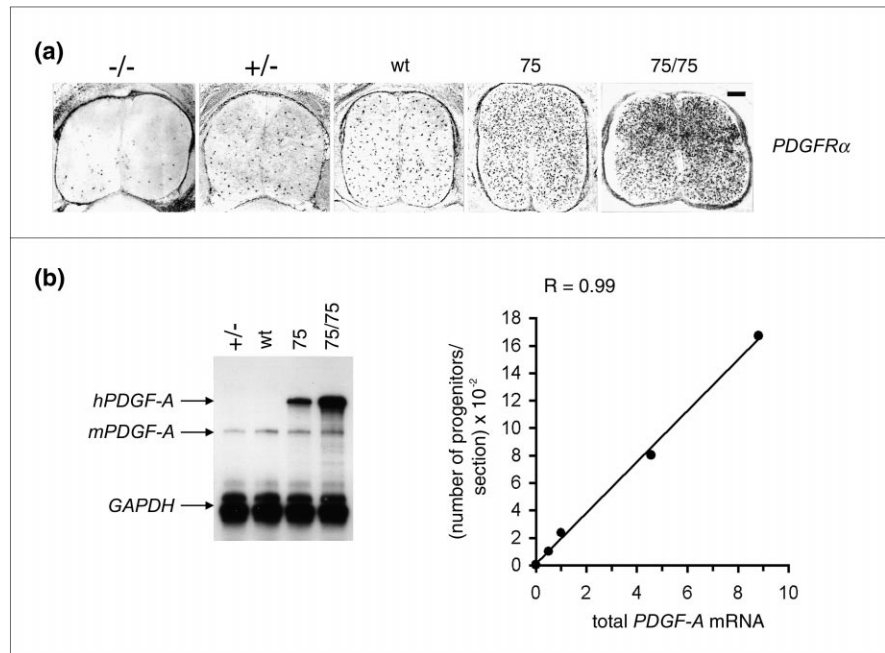
Discussion

Progenitor cell cycle dynamics and final cell number is controlled by the environment

One of the main conclusions of this work is that progenitor cell cycle dynamics (that is, the deceleration of the cycle observed as the embryo ages) is controlled by the extracel-

Figure 6

Progenitor cell number is proportional to the PDGF supply. The linear relationship between *PDGF-A* and final cell number also holds when PDGF is underexpressed in *PDGF-A* knockouts. **(a)** Spinal cord sections of E15 mouse embryos hybridized in situ to a *PDGFR α* probe: homozygous *PDGF-A* knockout (*-/-*), heterozygous *PDGF-A* knockout (*+/-*), wild type (*wt*), hemizygous *NSE-PDGF-A* (75), and homozygous *NSE-PDGF-A* (75/75). Progenitor cell numbers rise with increasing levels of *PDGF-A* expression. The scale bar represents 100 μ m. **(b)** Total *PDGF-A* mRNA level was estimated by RNase protection and plotted against the number of *PDGFR α* progenitors counted by eye in photographic enlargements of the in situ micrographs. The amount of functional *PDGF-A* mRNA was assumed to be zero in (*-/-*) embryos and half of normal in (*+/-*) embryos, since our RNase protection assay could not distinguish wild-type from nonfunctional, hybrid *PDGF-A-neo* transcripts in the knockouts. The dose response is linear (correlation coefficient $R = 0.99$). Taken together with Figure 5, we conclude that progenitor cell number is directly proportional to PDGF supply over a range of expression levels from near zero (*PDGF-A* null) to more than ten times normal (75,82/75,82 transgenic).



lular environment. This follows from our observation that the cell division rates of E13 and E17 progenitors were indistinguishable in vitro in saturating PDGF, even though their division rates in vivo were very different. Slowing of the cell cycle is accompanied by a decline in the rate of increase of progenitor cell number, so that the cell number reaches a plateau before birth and remains stable for some time after birth. It seems likely that cell cycle dynamics directly influence the final cell number and therefore that the cell number is controlled by the environment, not by a cell-intrinsic counting mechanism. This does not mean that the intracellular state of cells stays constant during embryogenesis, but that any intrinsic changes that might limit the proliferation rate are probably a consequence of the changing mitogenic environment outside the cell and remain reversible, at least for a few days (between E13 and E17).

The progenitor cell population in the embryonic cord can be expanded seemingly without limit, simply by increasing the rate of supply of PDGF. This strongly supports our conclusion that the only effective constraint on progenitor cell number in the embryonic cord is the extracellular mitogen supply, and raises the question of whether progenitor cells would proliferate indefinitely in vivo if an inexhaustible supply of PDGF could be provided. We could not approach this condition because higher levels of PDGF caused spinal deformity and killed the animals. It is striking that cell number is directly proportional to

PDGF transcript levels (which we take to be an indicator of the rate of PDGF synthesis and secretion) over a wide range of *PDGF* expression. This is perhaps counterintuitive, being that mitogen dose–response curves in vitro are typically sigmoidal in shape, rising from background to maximal (plateau) response over a limited range of concentrations, about a 10-fold range for oligodendrocyte progenitors and PDGF [12]. In vitro dose responses, however, usually record *rate of cell division* versus mitogen *concentration*, whereas our in vivo dose response reflects *final cell number* versus *rate of production* of mitogen. We do not know what the effective PDGF concentration is in vivo except that it is limiting (subsaturating).

It should be possible to estimate the effective concentration of PDGF from the measured cell cycle time in vivo, given that cell cycle time seems to be predictably related to the PDGF concentration in vitro (Figure 3). At E13, cell cycle time in vivo was comparable to that measured in vitro in the presence of 1 ng/ml PDGF-AA (~ 30 hr). Cell cycle time at E17 in vivo was ~ 100 hr, however, suggesting that the effective PDGF concentration is much less than 1 ng/ml by that time. We have not recapitulated a 100-hour cycle in vitro, because in very low concentrations of PDGF the cells tend to drop out of division and differentiate, as they do in the complete absence of PDGF. It would be interesting to see whether the combination of a low concentration of PDGF together with fibroblast growth factor, which is known to inhibit

oligodendrocyte differentiation *in vitro* [13], would be able to keep progenitors dividing slowly *in vitro*. Omitting thyroid hormone from the medium might also help [14].

It should be noted that overexpressing PDGF does not affect the final number of postmitotic, differentiated oligodendrocytes that accumulates after birth [3], despite the increased number of progenitor cells. This is because numbers of progenitors and oligodendrocytes are controlled separately, progenitors by the mitogenic effect of PDGF and oligodendrocytes by axon-derived survival factors [15]. Our previous experiments showed that the rate of oligodendrocyte production is elevated in *NSE-PDGF-A* mice but that the excess oligodendrocytes are removed by programmed cell death, leaving a normal number of mature, myelinating cells [3].

We previously estimated the average progenitor cell cycle time at steady state (E17) to be about 24 hr [3]. To explain how the cells could continue to divide once a day while their number remained constant, we had to invoke large-scale death and removal of newly formed cells, around 200 cells per 10- μ m section per day. The fact that we could not detect large numbers of dying oligodendrocyte lineage cells in the prenatal spinal cord was not perceived to be a problem, as dead cells are usually cleared rapidly. Our revised cell cycle time of \sim 100 hr at steady state, however, means that the scale of oligodendrocyte death in the prenatal spinal cord can now be revised downward to around 50 cells/section/day.

We do not understand why our previous estimates of cell cycle time (T_c) were 4-fold shorter than they should have been. The measured labeling index (L) after a single BrdU pulse at E17 was similar then and now (\sim 20%). We previously assumed an invariant S phase (T_s) of 4 hr; given that it now seems that the S phase is closer to 12 hr at E17 (Figure 1), this goes a long way toward explaining the discrepancy at E17 (since $T_c = T_s/L$). It does not explain, however, the discrepancy at E13, when $T_s \approx$ 5 hr (Figure 1). We tried without success to replicate our previous results using both our present and former experimental paradigms. We conclude that, whatever the source of error before, our present data are more reliable and should take precedence.

A mitogen depletion model of cell population growth

A simple explanation that fits our observations (though not the only explanation; see Potential role of antiproliferative factors, below) is that the proliferating cells limit their own proliferation by consuming the available PDGF. As the cells multiply, the rate at which they consume PDGF (by receptor binding and internalization) increases in proportion to cell number until the rate of consumption matches the fixed rate of supply. At this point, increased competition for PDGF prevents further proliferation. This

simple model explains the linear relationship between the rate of PDGF supply and the final cell number (Figures 5 and 6). It also explains why the cell cycle slows down as the cell number rises (Figure 1), because the shifting balance between PDGF supply and demand should cause the PDGF concentration to decrease with time. Finally, it explains why the ultimate rate of cell division is the same in normal mice and transgenic PDGF overexpressers (Figure 4), as the PDGF concentration should be determined solely by the relative rates of PDGF supply and consumption, which, according to the model, are always equal at steady state.

We tried to detect a decline in PDGF concentration *in vivo* by Western blotting. We were unable, however, to detect PDGF-A in embryonic spinal cord tissue (E12 to birth) from either wild-type or homozygous *NSE-PDGF-A* mice, using any of several antibodies against PDGF-A or an antibody against the Myc tag on the carboxy terminus of transgene-derived human PDGF-A (data not shown). We were also unable to detect PDGF-A by immunohistochemistry in spinal cord sections. In contrast, we were easily able to detect the product of another *PDGF* transgene encoding a nonsecreted form of PDGF-A that has an endoplasmic reticulum retention signal (KDEL) appended to its carboxy terminus, either by immunohistochemistry [3] or Western blot (data not shown). It is likely that PDGF is normally secreted rapidly after synthesis and is difficult to detect once it leaves the cell. We have in the past been able to detect PDGF immunoreactivity *in situ*, but only inside cells, not in the extracellular space [16].

We also tried to detect PDGF activity indirectly by visualizing activated PDGFR α on Western blots of newborn spinal cord, using antibodies against both the receptor and phosphotyrosine. Although we could easily detect PDGFR α protein, we could not detect autophosphorylation. We could readily detect phosphorylated receptors on NIH 3T3 cells that were cultured in the presence of 10 ng/ml PDGF-AA. We tentatively conclude that the level of receptor phosphorylation in oligodendrocyte progenitors *in vivo* is low relative to PDGF-stimulated 3T3 cells, again consistent with our conclusion that the effective PDGF concentration *in vivo* is very low.

It has been proposed before that dividing cells should limit their own proliferation by consuming mitogens, on the basis of mathematical modeling [17]. Moreover, Holley and Kiernan [18] showed that the final population density attained by fibroblasts in culture is proportional to the initial serum concentration, and interpreted this in terms of depletion of serum growth factors by the expanding cell population. This explanation is similar to, and sets an early precedent for, the *in vivo* mitogen depletion model we propose here.

Mitogen depletion could potentially explain other puzzling examples of cell number control. One example is mouse aggregation chimeras. If two (or more) mouse blastocysts are aggregated *in vitro* and introduced into a surrogate mother, the chimeric blastocyst forms an oversized embryo that implants into the uterine wall as normal. At the end of gestation, however, a normal-sized mouse is born. Size regulation occurs shortly after implantation, when there is a burst of rapid cell divisions that take the embryo to a predetermined target size after which the cell cycle slows down again [19]. The cells of oversized embryos divide less rapidly than normal during the post-implantation burst, allowing them to reach the target size at the same time as their normal-sized littermates and develop in parallel thereafter [19]. This behavior could be explained if, for example, there were some invariant population of cells at the implantation site that supplied mitogens at a fixed rate, irrespective of the number of cells in the embryo. The cells of the embryo would then regulate their own proliferation rate and population growth through competition for the limited mitogen supply. Another example is that of tetraploid amphibians, which contain half the normal number of double-sized cells [20]. The larger cells of the tetraploid might be expected to carry more mitogen receptors than normal and to consume mitogens at a correspondingly faster rate. Therefore, fewer cells should develop in the tetraploid before mitogens are depleted and cell division arrests.

Potential role of antiproliferative factors

Formally, however, our data do not allow us to distinguish between mitogen depletion and autocrine production of an antiproliferative agent(s). Both mechanisms would result in a decrease in effective mitogenic activity that is proportional to progenitor cell number. Antiproliferative factors certainly do participate in developmental growth control. For example, the TGF β superfamily member NDF-8/myostatin negatively regulates muscle growth during development by inhibiting cell proliferation and myofibril growth [21, 22]. Myostatin is expressed by skeletal muscle cells, but it is not known whether it acts in an autocrine, paracrine, or systemic mode. Myostatin null mice have excessive skeletal muscle mass, whereas heterozygous knockouts appear almost normal, suggesting that myostatin controls muscle growth in an all-or-nothing fashion, not in a graded way as described here for PDGF. One possibility is that myostatin normally inhibits muscle growth through a step reduction in the sensitivity of muscle progenitors to mitogenic stimulation; mitogen depletion could still be the mechanism that ultimately halts muscle progenitor cell proliferation. In any case, mitogen depletion and autocrine inhibition are not mutually exclusive.

Oligodendrocyte progenitors in culture are known to secrete self-inhibitory activity [23], one component of which

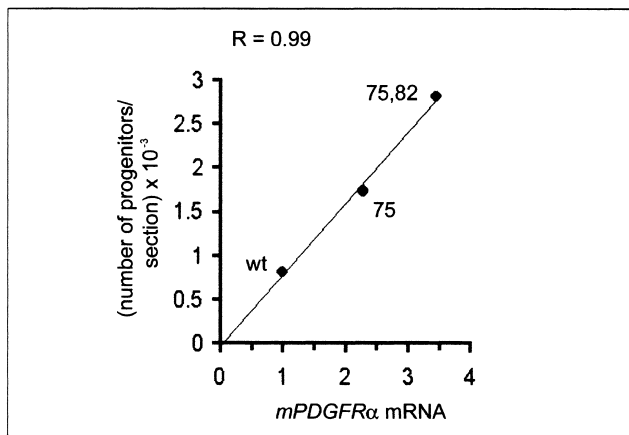
is TGF β 1 [24]. Thus, it is not unlikely that they produce autocrine inhibitors of cell proliferation *in vivo* too, although TGF β 1 itself does not seem to be important in this context because we found that progenitor cell numbers are normal in newborn TGF β 1 null mice (P.v.H., unpublished data) [25]. TGF β family members have their own specific cell surface receptors and intracellular signaling pathways. In some cells, under some conditions, (for example, fibroblasts cultured at a high cell density), TGF β 1 can inhibit the PDGF-mediated mitogenic response by a mechanism involving PDGF receptor downregulation [26]. Other types of inhibitors that could in principle play an autocrine role are PDGF binding proteins such as α_2 -microglobulin [27] or a receptor antagonist analogous to the Argos protein that inhibits epidermal growth factor signaling [28].

The role of the intracellular clock that times oligodendrocyte differentiation

There is known to be a cell-intrinsic mechanism that limits the proliferative lifetime of embryonic optic nerve oligodendrocyte progenitors cultured *in vitro* [29, 30]. This intracellular division limiter (clock) causes progenitor cells to lose responsiveness to PDGF, exit the cell cycle, and differentiate into oligodendrocytes after a fixed time *in vitro*, even when they are cultured continuously in saturating concentrations of PDGF [31]. It is thought that the primary function of the clock is to time the onset of oligodendrocyte differentiation around the time of birth, but in principle it could also influence progenitor cell number given that it stimulates cell cycle exit. Because oligodendrocytes do not start to appear in large numbers until after birth, however, the intracellular clock is unlikely to influence progenitor cell number noticeably in the embryo although it might have a greater effect in the postnatal period. It might be possible to test this by extending the kind of *in vivo* analysis described in this paper to postnatal ages.

Conclusions

First, for oligodendrocyte progenitors in the embryonic spinal cord, we have shown that the cell cycle rate and final number of cells is tightly controlled by the mitogenic environment in the cord, with no obvious contribution from cell-intrinsic limits on cell proliferation. Second, to explain the strict proportionality between PDGF expression and the steady-state number of progenitor cells, we suggest a simple mitogen depletion model, according to which the cells limit their own proliferation by consuming the available mitogens. The expanding cell population consumes mitogens at an increasing rate until the rate of consumption matches the fixed rate of supply. As a result, the mitogen concentration falls until it can no longer support proliferation. Other models are possible and might act in parallel. For example, the proliferating cells might secrete an autocrine inhibitor of their own proliferation. The common feature of these models is that cells modify

Figure 7

PDGFRα mRNA provides an accurate reflection of *PDGFRα*-positive progenitor cell number. *PDGFRα* transcripts in the spinal cords of newborn mice of the indicated genotypes were measured by RNase protection. *PDGFRα* mRNA abundance was plotted against progenitor cell number counted directly from spinal cord sections (data not shown). There is a linear relationship (correlation coefficient $R = 0.99$).

the mitogenic properties of their environment at a rate proportional to the total number of cells in the population.

Materials and methods

BrdU labeling in vivo

An osmotic minipump (Alza Corporation; 1 μ l/hr delivery rate) containing BrdU (180 mg/ml in 1% (w/v) ammonia solution) was inserted subcutaneously into a pregnant mouse to deliver BrdU at \sim 180 μ g/hr. Thus, it takes over 8 hr to deliver the same amount of BrdU as would a single injection at the usual dose of 50 μ g BrdU per gram body weight (around 30 g for a pregnant female). The latter method of delivery has been shown to be nontoxic for neurons in the developing cerebral cortex at E14 [32]. To determine whether our labeling regimen was adequate to visualize all dividing cells, we compared the BrdU labeling index of progenitors after the implantation of either one or three minipumps. With three pumps the BrdU-labeled cells appeared brighter, but the calculated labeling index was unchanged.

After labeling, embryonic or pup spinal cords were dissected, and dissociated cells cultured overnight in a defined medium [33] as described previously [6]. Omitting thyroxine and triiodothyronine from the medium in control experiments (data not shown) had no significant effect on cell cycle kinetics, and therefore the fully supplemented medium was used for all experiments reported here. Coverslips were labeled with anti-NG2 chondroitin sulfate proteoglycan (Chemicon International) and anti-BrdU (monoclonal BU209) [34] followed by the appropriate fluorescein- or rhodamine-conjugated secondary antibodies. Labeled cells were counted in a fluorescence microscope and the labeling index (the fraction of NG2-positive oligodendrocyte progenitors that was also BrdU positive) was calculated. For each time point, at least 200 NG2-positive cells on each of three or more coverslips were scored. Alternatively, spinal cord sections were subjected to combined BrdU immunohistochemistry and in situ hybridization with a probe against mouse *PDGFRα* to identify labeled oligodendrocyte progenitors. Both methods yielded similar labeling indices at E13, so immunolabeling of dissociated cells was used in all further experiments. Control experiments (data not shown) confirmed that, in spinal cord cultures, 100% of *PDGFRα*-immunoreactive process-

bearing cells were also NG-2 immunoreactive, and more than 95% of NG-2-positive cells were *PDGFRα* positive.

BrdU labeling in vitro

Spinal cords were cultured as described previously [6], with PDGF-AA (ImmunoKontakt, Frankfurt, Germany) at various concentrations. In mixed-age cultures, cells of one age were marked before mixing by incubating in 1 μ M carboxyfluorescein diacetate, succinimidyl ester (CFSE, Molecular Probes) in the dark at room temperature, followed by thorough washing. The stock was 1 mM CFSE in dimethyl sulfoxide. After culturing overnight, 10 μ M BrdU was added and the incubation was continued at 37°C. Coverslips were removed at various times and the BrdU labeling index was determined as above.

Cell cycle analysis by cumulative BrdU labeling

For a uniformly cycling population of cells exposed continuously to BrdU, the fraction of BrdU-labeled cells (labeling index, L) increases linearly with time until all cells are labeled ($L = 1$). By plotting L versus time of BrdU exposure, the total cell cycle time (T_c) and S phase time (T_s) can be deduced by the formulae ($T_c = 1/m$) and ($T_s = n/m$), where m is the gradient and n is the intercept on the L axis (that is, the labeling index after a single short pulse of BrdU) [32].

We calculated the line of best fit and standard errors for m and n by the method of least squares, then the 67% confidence intervals (p_m and p_n) by multiplying the standard errors by the t value of the two-tailed Student's t distribution for probability 0.33 ($N-2$ degrees of freedom) [35]. From these, we calculated the corresponding 67% confidence intervals for T_c and T_s . Because T_c and T_s are calculated from the reciprocal of m , the confidence intervals are not symmetrical about the mean, but for convenience, we quote the experimental errors for T_c and T_s as \pm half the full range. Each cumulative labeling experiment was repeated at least twice with similar results. One representative experiment is shown in each case.

Transgenic mice

Production and genotyping of transgenic *NSE-PDGF-A* mice and *PDGF-A* knockout mice has been described [8]. *NSE-PDGF-A* lines #75 and #82 can be distinguished on Southern blots by the different sizes of junction fragments produced by BamHI digestion of genomic DNA. To distinguish hemizygous and homozygous transgenics, band intensity was quantified using a phosphorimager (Packard). To generate offspring with different combinations of transgene loci (for Figure 5), we crossed male and female double-hemizygous 75,82/+,+ mice.

Tissue preparation and in situ hybridization

Tissue preparation and in situ hybridization was done as described previously [11]. Cryosections were cut at a 10- μ m nominal thickness. The *PDGF-A* antisense probe was transcribed from a 68-bp EcoRI-HindIII fragment encompassing most of the human *PDGF-A* cDNA [36] cloned into pBluescript-SK (Stratagene). The plasmid was linearized with EcoRI and transcribed with T7 RNA polymerase (T7pol). The *PDGFRα* probe was transcribed from a 1636-bp EcoRI fragment encoding most of the extracellular domain of mouse *PDGFRα* [37] cloned into pBluescript-KS. The plasmid was linearized with HindIII and transcribed with T7pol. In some experiments, *PDGFRα*-positive progenitors were counted in high-magnification photographic prints of in situ hybridization micrographs.

RNase protection assay

mRNA expression was analyzed by RNase protection [38] using the cDNAs described above for the preparation of 32 P-labeled riboprobes. Protected RNA fragments were separated on a 6% (w/v) polyacrylamide-sequencing gel. Band intensities were measured using a phosphorimager and, after background subtraction, each value was normalized against mRNA levels for the housekeeping gene *GAPDH*. A control experiment showed that *PDGFRα* mRNA abundance gives an accurate reflection of oligodendrocyte progenitor cell number (Figure 7).

Acknowledgements

We thank our colleagues past and present for help and encouragement. We also thank Christer Betsholtz (University of Göteborg, Sweden) and John Heath (University of Birmingham, UK) for the *PDGF-A* knockout mice, and Martin Raff for helpful comments on the manuscript. This work was supported by the Medical Research Council and the Multiple Sclerosis Society of Great Britain and Northern Ireland.

References

- Conlon I, Raff M: **Size control in animal development.** *Cell* 1999, **96**:235-244.
- Slack JM: **Growth control: action mouse.** *Curr Biol* 1997, **7**:467-469.
- Calver AR, Hall AC, Yu WP, Walsh FS, Heath JK, Betsholtz C, *et al.*: **Oligodendrocyte population dynamics and the role of PDGF in vivo.** *Neuron* 1998, **20**:869-882.
- Takahashi T, Nowakowski RS, Caviness VS Jr: **The cell cycle of the pseudostratified ventricular epithelium of the embryonic murine cerebral wall.** *J Neurosci* 1995, **15**:6046-6056.
- Pringle NP, Richardson WD: **A singularity of PDGF α -receptor expression in the dorsoventral axis of the neural tube may define the origin of the oligodendrocyte lineage.** *Development* 1993, **117**:525-533.
- Hall A, Giese NA, Richardson WD: **Spinal cord oligodendrocytes develop from ventrally-derived progenitor cells that express PDGF α -receptors.** *Development* 1996, **122**:4085-4094.
- Nishiyama A, Lin XH, Giese N, Heldin CH, Stallcup WB: **Co-localization of NG2 proteoglycan and PDGF α -receptor on O2A progenitor cells in the developing rat brain.** *J Neurosci Res* 1996, **43**:299-314.
- Fruttiger M, Calver AR, Kruger WH, Mudhar HS, Michalovich D, Takakura N, *et al.*: **PDGF mediates a neuron-astrocyte interaction in the developing retina.** *Neuron* 1996, **17**:1117-1131.
- van Heyningen P: *Control of glial progenitor cell number in the developing central nervous system.* PhD Thesis. University of London, UK: 2000.
- Boström H, Willetts K, Pekny M, Leveén P, Lindahl P, Hedstrand H, *et al.*: **PDGF-A signaling is a critical event in lung alveolar myofibroblast development and alveogenesis.** *Cell* 1996, **85**:863-873.
- Fruttiger M, Karlsson L, Hall AC, Abramsson A, Calver AR, Bostrom H, *et al.*: **Defective oligodendrocyte development and severe hypomyelination in PDGF-A knockout mice.** *Development* 1999, **126**:457-467.
- Richardson WD, Pringle N, Mosley MJ, Westermark B, Dubois-Dalcq M: **A role for platelet-derived growth factor in normal gliogenesis in the central nervous system.** *Cell* 1988, **53**:309-319.
- Bogler O, Wren D, Barnett SC, Land H, Noble M: **Cooperation between two growth factors promotes extended self-renewal and inhibits differentiation of oligodendrocyte-type-2 astrocyte (O-2A) progenitor cells.** *Proc Natl Acad Sci USA* 1990, **87**:6368-6372.
- Barres BA, Lazar MA, Raff MC: **A novel role for thyroid hormone, glucocorticoids and retinoic acid in timing oligodendrocyte development.** *Development* 1994, **120**:1097-1108.
- Barres BA, Raff MC: **Axonal control of oligodendrocyte development.** *J Cell Biol* 1999, **147**:1123-1128.
- Mudhar HS, Pollock RA, Wang C, Stiles CD, Richardson WD: **PDGF and its receptors in the developing rodent retina and optic nerve.** *Development* 1993, **118**:539-552.
- Sulzer B, Perelson AS: **Equilibrium binding of multivalent ligands to cells: effects of cell and receptor density.** *Math Biosci* 1996, **135**:147-185.
- Holley RW, Kiernan JA: **"Contact inhibition" of cell division in 3T3 cells.** *Proc Natl Acad Sci USA* 1968, **60**:300-304.
- Lewis NE, Rossant J: **Mechanism of size regulation in mouse embryo aggregates.** *J Embryol Exp Morphol* 1982, **72**:169-181.
- Fankhauser G: **Nucleo-cytoplasmic relations in amphibian development.** *Int Rev Cytol* 1952, **1**:165-193.
- McPherron AC, Lawler AM, Lee SJ: **Regulation of skeletal muscle mass in mice by a new TGF- β superfamily member.** *Nature* 1997, **387**:83-90.
- Lee SJ, McPherron AC: **Myostatin and the control of skeletal muscle mass.** *Curr Opin Genet Dev* 1999, **9**:604-607.
- Louis JC, Muir D, Varon S: **Autocrine inhibition of mitotic activity in cultured oligodendrocyte-type-2 astrocyte (O-2A) precursor cells.** *Glia* 1992, **6**:30-38.
- McKinnon RD, Piras G, Ida JA Jr, Dubois-Dalcq M: **A role for TGF- β in oligodendrocyte differentiation.** *J Cell Biol* 1993, **121**:1397-1407.
- Kulkarni AB, Huh CG, Becker D, Geiser A, Lyght M, Flanders KC, *et al.*: **Transforming growth factor β 1 null mutation in mice causes excessive inflammatory response and early death.** *Proc Natl Acad Sci USA* 1993, **90**:770-774.
- Paulsson Y, Karlsson C, Heldin CH, Westermark B: **Density-dependent inhibitory effect of transforming growth factor- β 1 on human fibroblasts involves the down-regulation of platelet-derived growth factor α -receptors.** *J Cell Physiol* 1993, **157**:97-103.
- Huang JS, Huang SS, Deuel TF: **Specific covalent binding of platelet-derived growth factor to human plasma α 2-macroglobulin.** *Proc Natl Acad Sci USA* 1984, **81**:342-346.
- Schweitzer R, Howes R, Smith R, Shilo BZ, Freeman M: **Inhibition of *Drosophila* EGF receptor activation by the secreted protein Argos.** *Nature* 1995, **376**:699-702.
- Temple S, Raff MC: **Clonal analysis of oligodendrocyte development in culture: evidence for a developmental clock that counts cell divisions.** *Cell* 1986, **44**:773-779.
- Durand B, Fero ML, Roberts JM, Raff MC: **p27^{Kip1} alters the response of cells to mitogen and is part of a cell-intrinsic timer that arrests the cell cycle and initiates differentiation.** *Curr Biol* 1998, **8**:431-440.
- Raff MC, Lillien LE, Richardson WD, Burne JF, Noble MD: **Platelet-derived growth factor from astrocytes drives the clock that times oligodendrocyte development in culture.** *Nature* 1988, **333**:562-565.
- Nowakowski RS, Lewin SB, Miller MW: **Bromodeoxyuridine immunohistochemical determination of the lengths of the cell cycle and the DNA-synthetic phase for an anatomically defined population.** *J Neurocytol* 1989, **18**:311-318.
- Bottenstein JE, Sato GH: **Growth of a rat neuroblastoma cell line in serum-free supplemented medium.** *Proc Natl Acad Sci USA* 1979, **76**:514-517.
- Magaud JP, Sargent I, Clarke PJ, Ffrench M, Rimokh R, Mason DY: **Double immunocytochemistry labelling of cell and tissue samples with monoclonal anti-bromodeoxyuridine.** *J Histochem Cytochem* 1989, **37**:1517-1527.
- Brown D, Rothery P: *Models in Biology: Mathematics, Statistics and Computing.* Chichester, UK: John Wiley and Sons; 1993.
- Betsholtz C, Johnsson A, Heldin C-H, Westermark B, Lind P, Urdea MS, *et al.*: **cDNA sequence and chromosomal localization of human platelet-derived growth factor A-chain and its expression in human tumour cell lines.** *Nature* 1986, **320**:695-699.
- Palmieri SL, Payne J, Stiles CD, Biggers JD, Mercola M: **Expression of mouse PDGF-A and PDGF α -receptor genes during pre- and post-implantation development: evidence for a developmental shift from an autocrine to a paracrine mode of action.** *Mech Dev* 1992, **39**:181-191.
- Melton DA, Krieg PA, Rebagliati MR, Maniatis T, Zinn K, Green MR: **Efficient in vitro synthesis of biologically active RNA and RNA hybridization probes from plasmids containing a bacteriophage SP6 promoter.** *Nucleic Acids Res* 1984, **12**:7035-7056.